



Co-incorporating enhancement on oxygen vacancy formation energy and electrochemical property of $\text{Sr}_2\text{Co}_{1-x}\text{Mo}_{1-x}\text{O}_{6-\delta}$ cathode for intermediate-temperature solid oxide fuel cell



Wenwen Zhang^{a,b}, Junling Meng^a, Xiong Zhang^{a,b}, Lifang Zhang^{a,b}, Xiaojuan Liu^{a,*}, Jian Meng^a

^a State Key Laboratory of Rare Earth Resource Utilization, Changchun Institute of Applied Chemistry, Chinese Academy of Sciences, Changchun 130022, PR China

^b University of Science and Technology of China, Hefei, Anhui 230026, PR China

ARTICLE INFO

Keywords:

Solid oxide fuel cells
Cathode
First-principles calculation
Oxygen vacancy
Electrochemical performance

ABSTRACT

Theoretical and experimental endeavor were combined to investigate effects of Co-incorporating on crystal structure and oxygen vacancy formation energy and their influence on $\text{Sr}_2\text{Co}_{1-x}\text{Mo}_{1-x}\text{O}_{6-\delta}$ electrochemical performance systematically. From the X-ray diffraction (XRD) and X-ray photoelectron spectroscopy (XPS), it is found that introducing Co decreases the ordering of B-site cations. Most importantly, Co^{3+} content increases with the increasing Co, indicating more Co-O* pairs are introduced within the compounds. Additionally note that the electrochemical performance of the materials is improved apparently when more Co is incorporated. $\text{Sr}_2\text{Co}_{1.5}\text{Mo}_{0.5}\text{O}_{6-\delta}$ has an area-specific polarization resistance (ASR) as low as $0.030 \Omega \text{ cm}^2$ in a symmetrical cell at 800°C . First-principles calculations found that the sequence of the oxygen vacancy formation energy was $\text{Co-O}^* \text{-Co} < \text{Co-O}^* \text{-Mo}$, indicating that Co-doping facilitates formation of oxygen vacancy, which coincides well with experimental results. Therefore, Co-incorporating in $\text{Sr}_2\text{CoMoO}_6$ is an efficient way to enhance electrochemical performance of cathode for IT-SOFCs.

1. Introduction

Solid oxide fuel cells (SOFCs) have great potential to be an alternative to traditional fire-power plants for generating electricity due to efficient chemical-to-electrical energy conversion, low emissions and outstanding fuel flexibility [1–4]. However, the high cost and limited system life arising from high operating temperature hampers widespread commercialization of SOFCs technology [3]. The sluggish kinetics of the oxygen reduction reaction (ORR) at cathode degrades overall cell performance, particularly at lower temperature [3–6]. Therefore, the development of novel cathode materials with good catalytic activity for ORR and durability is crucial for practical applications of SOFCs at intermediate temperatures [6,7].

During the past decades, intensive studies have been devoted to the exploration for more active cathode materials toward ORR at intermediate temperatures ($600\text{--}800^\circ\text{C}$). The mixed ionic and electronic conductivities (MIECs) have been attracted tremendous attention because of their extended active sites toward ORR when compared with purely electronic conducting materials [6–8]. Among these MIECs cathode, cobalt-based perovskite-type oxides, such as $\text{Ba}_{0.5}\text{Sr}_{0.5}\text{Co}_{0.8}\text{Fe}_{0.2}\text{O}_{3-\delta}$ [4], $\text{La}_{0.6}\text{Sr}_{0.4}\text{Co}_{1-x}\text{Fe}_x\text{O}_{3-\delta}$ [9],

$\text{PrBa}_{0.5}\text{Sr}_{0.5}\text{Co}_{2-x}\text{Fe}_x\text{O}_{5+\delta}$ [10] and $\text{SrCo}_{0.8}\text{Nb}_{0.1}\text{Ta}_{0.1}\text{O}_{3-\delta}$ [11], were considered to be the most promising cathode candidates owing to the high ionic and electronic conductivity. Nevertheless, central to cobalt-based oxides is the mismatch in thermal expansion coefficients (TECs) between the electrode and electrolyte, which restricts their practical use. It is reported that the Co-based double perovskite oxide $\text{Sr}_2\text{CoMoO}_6$ exhibits a low TECs of 6×10^{-6} to $15 \times 10^{-6} \text{ K}^{-1}$ between room temperature (RT) and 900°C , matching well with those of SDC and LSGM electrolyte ($10\text{--}13 \times 10^{-6} \text{ K}^{-1}$) [12–15]. To our knowledge, it is suitable for $\text{Sr}_2\text{CoMoO}_6$ system to be anode or cathode, and it shows an outstanding electrochemical performance when used as anode materials. However, few reports about the research that $\text{Sr}_2\text{CoMoO}_6$ system is used as cathode materials. It has been expected that Co doping on Mo sites would remarkably enhance both the ionic and electronic conductivity due to variable valence state of Co ions. Furthermore, the effects of Co doping on structures and cathode performance of $\text{Sr}_2\text{Co}_{1-x}\text{Mo}_{1-x}\text{O}_{6-\delta}$ for intermediate-temperature solid oxide fuel cell has not yet been studied.

Herein, we designed a series of Co-rich double perovskite oxides $\text{Sr}_2\text{Co}_{1-x}\text{Mo}_{1-x}\text{O}_{6-\delta}$ ($\text{SC}_{1-x}\text{M}_1\text{O}_{6-\delta}$, $x = 0.0, 0.3, 0.5$) in which Mo ions are partially substituted by Co ions. And effects of Co

* Corresponding author.

E-mail address: lxjuan@ciac.ac.cn (X. Liu).

substitution of Mo on B-site ordering, element valence, thermal expansion behaviors, ionic and electronic conductivity of $\text{SC}_{1+x}\text{M}_{1-x}\text{O}$ system have been systematically investigated. It can be observed that the Co-incorporating has significant positive influences on electrochemical performance of materials. And influence of Co-doping on oxygen vacancy formation energy is discussed in detail. Also, oxygen vacancy formation energy of materials is obtained by the first-principles calculation. It is found that introducing Co decreases oxygen vacancy formation energy of materials tremendously, which is consistent with the experimental results.

2. Experimental

2.1. Sample synthesis

$\text{Sr}_2\text{Co}_{1+x}\text{Mo}_{1-x}\text{O}_{6-\delta}$ ($\text{SC}_{1+x}\text{M}_{1-x}\text{O}$, $x = 0, 0.3, 0.5$) was prepared through a sol-gel route. Analytical reagents of $\text{Sr}_2(\text{NO}_3)_2$, $\text{Co}(\text{NO}_3)_2 \cdot 6\text{H}_2\text{O}$, $(\text{NH}_4)\text{Mo}_7\text{O}_{24} \cdot 4\text{H}_2\text{O}$ were used as the starting materials. The stoichiometric quantities of above raw materials were dissolved into de-ionized water. An appropriate amount of citric acid and polyethylene glycol were subsequently added as complexing agents under vigorous stirring to achieve a clear dull-red solution. Then the solution was slowly vaporized in the water bath at 90°C overnight. The obtained gel was heated in an oven for spontaneous combustion. The as-prepared powders were first sintered at 900°C in air for 10 h to remove organic matter. The precursors were pelletized and ultimately calcined at 1200°C in air for 10 h to obtain the pure phase. The $\text{La}_{0.9}\text{Sr}_{0.1}\text{Ga}_{0.8}\text{Mg}_{0.2}\text{O}_{3-\delta}$ (LSGM) electrolyte powders and $\text{Ce}_{0.8}\text{Sm}_{0.2}\text{O}_{2-\delta}$ (SDC) buffer layer were synthesized in the same way.

2.2. Cell fabrication

Symmetrical cells with a $\text{SC}_{1+x}\text{M}_{1-x}\text{O}|\text{LSGM}|\text{SC}_{1+x}\text{M}_{1-x}\text{O}$ configuration were fabricated by screen-printing technique for electrochemical testing. Dense LSGM pellets (15 mm diameter) were prepared by dry pressing with subsequent isostatic cool pressing, and finally sintered at 1450°C in air for 10 h. The electrode slurries were prepared by mixing the powders with binder (α -terpineol and ethylene cellulose) and screen-printed on both sides of the LSGM with 500 μm thickness symmetrically, followed by burning at 1100°C in air for 2 h. Ag paste was painted in a grid structure as the current collector. The single-cell performance of $\text{SC}_{1+x}\text{M}_{1-x}\text{O}$ was tested with the cell configuration of $\text{NiO-SDC}|\text{SDC}|\text{LSGM}|\text{SC}_{1+x}\text{M}_{1-x}\text{O}$. The LSGM pellets were polished to a thickness of 300 μm . With $\text{NiO} + \text{SDC}$ (the weight ratio of NiO to SDC is 65 wt%:35 wt%) as anode, anode slurry was screen-printed on the SDC-coated LSGM electrolyte. Then $\text{SC}_{1+x}\text{M}_{1-x}\text{O}$ ink was applied as a cathode in the same way with symmetrical cells and finally fired at 1100°C in air for 2 h.

2.3. Characterizations

The initial phase structure of $\text{SC}_{1+x}\text{M}_{1-x}\text{O}$ powders was characterized by X-ray diffraction (XRD) in a Bruker AXS D8 Advance diffractometry (40 kV, 40 mA) with $\text{Cu-K}\alpha$ radiation ($\lambda = 1.5418 \text{ \AA}$), and adopted a scan rate of 8° min^{-1} in the 2θ range of $10\text{--}90^\circ$. The Rietveld refinements data of samples was collected using a Rigaku D/max-2500 diffractometer (40 kV, 200 mA) with $\text{Cu K}\alpha$ radiation ($\lambda = 1.5418 \text{ \AA}$) and employed a step-scan mode over a range of $10\text{--}120^\circ$ with intervals of 0.02° . The Rietveld refinements of the samples were performed using GSAS-EXPGUI software. The oxidation state of the elements in $\text{SC}_{1+x}\text{M}_{1-x}\text{O}$ samples was examined by X-ray photoelectron spectroscopy (XPS, VG ESCALAB 250). Hitachi S-4800 high resolution FE-SEM equipped with the energy dispersive X-ray spectrometer (EDS) analyzer (XP30, Philips) was used to observe the morphology. The thermogravimetric analysis of the material was operated on a NETZSCH STA 449F3 under air atmosphere from room temperature to 1000°C at

$10^\circ\text{C min}^{-1}$. Thermal expansion data were collected with a dilatometer (NETZSCH DIL 402C) under air atmosphere at a rate of 3°C min^{-1} between 50°C and 850°C . The electrical conductivity was measured in air from 850°C to 200°C with a Van der Pauw four-terminal dc method on a Keithley 2400 SourceMeter. The polarization resistance of symmetrical cell was tested by Autolab Electrochemical Instruments PGSTAT302 between 850°C and 650°C . The frequency applied to electrochemical impedance spectroscopy (EIS) was ranged from 0.01 Hz to 1 MHz with an amplitude signal of 10 mV. To investigate electrochemical performance of the single cell, humidified hydrogen fuel was fed into the anode at a flow rate of 100 mL min^{-1} , and ambient air served as the oxidant gas in the cathode.

2.4. First principles calculation

To get insight into the effect of Co-doping on oxygen vacancy formation energy and conductivity of $\text{Sr}_2\text{Co}_{1+x}\text{Mo}_{1-x}\text{O}_{6-\delta}$ cathode, first principles calculations were performed in the present work. The structure model of the $\text{Sr}_2\text{Co}_{1+x}\text{Mo}_{1-x}\text{O}_{6-\delta}$ compounds were based on the $I4/m$ (No. 87) tetragonal $\text{Sr}_2\text{CoMoO}_6$ conventional cell, meanwhile, $5 \times 1 \times 1$ supercells were built, in which there are 100 atoms for the compounds without oxygen vacancy, and 99 atoms for the compound with the oxygen vacancy concentration of $\delta = 0.1$. All calculations reported in this work were carried out using the VASP code (version 5.2.2) [16,17]. The nuclei and core electrons were represented within the frozen-core projector-augmented wave [18,19] approach using standard potentials for Co ($4s^23d^7$), Mo ($4p^65s^14d^5$), Sr ($4s^24p^65s^2$), and regular O ($2s^22p^4$) from the VASP library, where the outer core/valence electrons shown in parentheses are self-consistently optimized [19]. The generalized gradient approximation (GGA) method [20,21] with the parameterization of Perdew-Burke-Ernzerhof revised for solids (PBEsol) [21] was used for exchange and correlation functional. A $1 \times 4 \times 3$ Monkhorst-Pack k-point mesh was applied to $\text{Sr}_{20}\text{Co}_{10}\text{Mo}_{10}\text{O}_{60}$, $\text{Sr}_{20}\text{Co}_{13}\text{Mo}_7\text{O}_{60}$, $\text{Sr}_{20}\text{Co}_{15}\text{Mo}_5\text{O}_{60}$, $\text{Sr}_{20}\text{Co}_{10}\text{Mo}_{10}\text{O}_{59}$, $\text{Sr}_{20}\text{Co}_{13}\text{Mo}_7\text{O}_{59}$, and $\text{Sr}_{20}\text{Co}_{15}\text{Mo}_5\text{O}_{59}$ supercells. Each crystal structure was fully relaxed with the plane-wave energy cutoff of 550 eV under the conduction of residual force $\leq 0.05 \text{ eV/\AA}$.

3. Results and discussion

3.1. Structural analysis

Fig. 1 shows the XRD patterns of as-synthesized $\text{Sr}_2\text{Co}_{1+x}\text{Mo}_{1-x}\text{O}_{6-\delta}$ ($x = 0.0, 0.3, 0.5$) oxides. As can be seen, single-phase materials were synthesized successfully for all the samples and no detectable impurity phase. Besides, the chemical compatibility

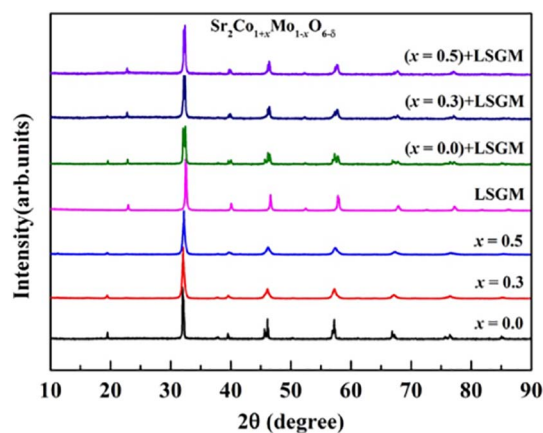


Fig. 1. XRD patterns of the as-synthesized $\text{Sr}_2\text{Co}_{1+x}\text{Mo}_{1-x}\text{O}_{6-\delta}$ ($x = 0.0, 0.3$ and 0.5) powders and the compounds of $\text{SC}_{1+x}\text{M}_{1-x}\text{O}_{6-\delta}$ series with LSGM calcined at 1000°C for 10 h in air.

Download English Version:

<https://daneshyari.com/en/article/7744559>

Download Persian Version:

<https://daneshyari.com/article/7744559>

[Daneshyari.com](https://daneshyari.com)